Theoretical Studies of Benzonitrile at the Si(100)-2×1 Surface

Yong-Quan Qu and Ke-Li Han*

Center for Computational Chemistry, Dalian Institute of Chemical Physics, Chinese Academy of Sciences, Dalian, People's Republic of China 116023

Received: January 14, 2004; In Final Form: March 18, 2004

Motivated by the selective binding of multifunctional organic molecules at the semiconductor surfaces, theoretical calculations of benzonitrile at the Si(100)-2×1 surface are carried out in order to explore the principles that control the competition and selectivity of surface reactions between the phenyl ring and the cyano group. B3LYP density functional theory with a Si_9H_{12} one-dimer cluster model is used to mimic surface reactions. The possible pathways of C2═C1−C≡N [4 + 2] cycloaddition, C≡N [2 + 2] cycloaddition, C═C [2 + 2] cycloaddition, C═C [4 + 2] cycloaddition, and C−H dissociation are investigated. The calculations illustrate that C≡N [2 + 2] cycloaddition is the selective pathway for chemisorbed benzonitrile at the Si (100)-2×1 surface.

Introduction

Recently, there has been a surging interest in abilities to controllably attach multifunctional compounds to semiconductor surfaces, because it is a crucial step toward applications in the areas of hybrid organic−semiconductor devices, biological recognition, nanotechnology, and so on.[1−14] Many organic molecules, such as ketones, amino acids, nitrile compounds, and aromatic compounds, have been tested to explore the principles that control the possible reactions at the semiconductor surfaces.[6−14] Previous studies have shown that some organic molecules containing more than one functional group did not create a high degree order at the semiconductor surfaces, possibly because different functional groups of a molecule can complete and lead to nonselective bonding at the semiconductor surfaces. Fundamental understanding of the attachment chemistry of organic molecules at semiconductor surfaces is still a challenging topic in functionalization of semiconductor surfaces.

Of particular interest is the Si(100) surface, which undergoes 2 × 1 reconstruction and forms rows of dimers under proper conditions. The special electronic characteristics of the Si(100) surface dimers lead to two main classes of surface reactions that have analogies in classic organic chemistry. Each dimer contains a strong σ bond and a weak π bond,[15] making it structurally and electronically similar to some of the characteristics of classical alkenes from organic chemistry. Diels−Alder and [2 + 2] cycloaddition products via the surface reactive sites have been demonstrated experimentally and theoretically to attach organic molecules at the semiconductor surfaces. On the other hand, due to solid-state electronic effects, surface dimers dynamically tilt out of the surface plane,[16] associated with a charge transfer from the "down" silicon atom to the "up" silicon atom, which adds zwitterionic effects to the dimers. Therefore, the electron-deficient down silicon atom and electron-rich silicon atom can act as electron acceptor and electron donors, respectively. Lewis acid−base reaction is expected at the Si(100)-2×1 surface.

The covalent binding of benzene at the Si(100)-2×1 surface has been well-demonstrated. The majority surface product of benzene[17−22] is a [4 + 2] cycloaddition structure involving 1,4 carbon atoms of benzene and the surface dimer. The known change in reactivity of substituent groups on aromatic molecules has spurred the investigations on benzene derivations, such as styrene,[23] aniline,[24−26] phenyl isothiocyanate,[27] benzonitrile,[28] benzoic acid,[24] and benzenethiol.[29] These organic molecules are observed to react with the surface dimers through the substituent groups, leaving the phenyl ring intact.

Since many of the proposed applications require the selective adsorption of a monolayer, it is crucial to understand the principles that govern competition and selectivity of multifunctional organic molecules at semiconductor surfaces. Nitrile compounds with a large dipole moment have been proposed as promising candidates for molecular layer growth of organic compounds at semiconductor surfaces. Chemisorption of nitrile compounds at the semiconductor surface, such as acetonitrile and 2-propenenitrile, have been intensively investigated by various experimental techniques and theoretical calculations.[30−35] In this paper, we carry out ab initio calculations on benzonitrile at the Si(100)-2×1 surface and investigate the substituent effects. Benzonitrile contains a conjugated cyano and phenyl ring, and rich adsorption chemistry at the Si(100)-2×1 surface can be expected as shown in Figure 1.

Computational Methods

The clean Si(100)-2×1 surface is represented by a Si_9H_{12} cluster consisting of four layers of silicon atoms. The Si_9H_{12} one-dimer cluster includes the two silicon atoms in the top layer comprising the surface dimer, four second-layer silicon atoms, two third-layer silicon atoms, and one fourth-layer silicon atom. The subsurface dangling bonds of the cluster are terminated by hydrogen atoms in order to preserve the sp^3 bonding characteristics of the subsurface silicon atoms and avoid the nonphysical effects that stem from subsurface dangling bond. However, the electronegativity difference between silicon and hydrogen may create a chemical environment at the cluster boundary that is different from the actual Si(100)-2×1 surface. Widjaja and Musgrave[36] have used the cluster model of various sizes to determine that the error caused by the terminating hydrogen is insignificant.

* To whom correspondence should be addressed. E-mail: klhan@dicp.ac.cn.

10.1021/jp049797x CCC: $27.50
Published on Web 05/20/2004

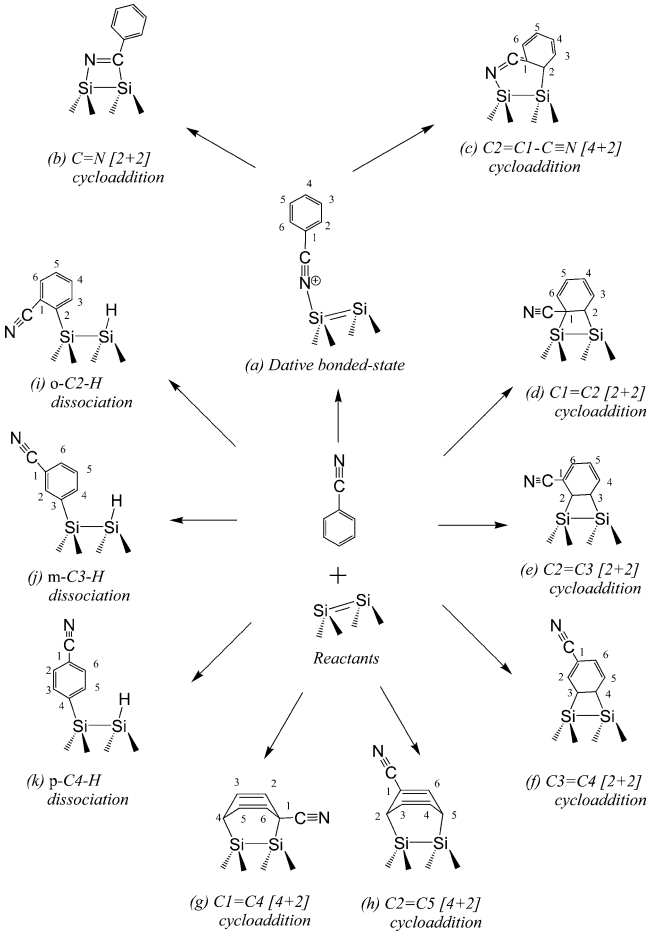

Figure 1. Possible surface reaction pathways of benzonitrile at the Si(100)-2×1 surface: (a) dative-bonded state; (b) C≡N [2 + 2] cycloaddition; (c) C2−C1−C≡N [4 + 2] cycloaddition; (d) C1═C2 [2 + 2] cycloaddition; (e) C2═C3 [2 + 2] cycloaddition; (f) C3═C4 [2 + 2] cycloaddition; (g) C1═C4 [4 + 2] cycloaddition; (h) C2═C5 [4 + 2] cycloaddition; (i) *o*-C2−H dissociation; (j) *m*-C3−H dissociation; and (k) *p*-C4−H dissociation.

In this work, we use the B3LYP[37−39] three-parameter gradient corrected hybrid density functional theory (DFT[40,41]) method for all electronic structures with the Gaussian 98[42] software package. The geometries of all minima and transition states in the potential energy surfaces in this work were calculated at the B3LYP/6-31G(d) level of theory without applications of geometry constraints or symmetry restrictions on the clusters. All calculated transition states on the potential energy surfaces were verified by frequency calculations to have one and only one imaginary frequency and followed by intrinsic reaction coordinate (IRC) calculations. Single-point energy calculations were performed on the optimized structures at the B3LYP level of theory with a mixed basis set scheme. The mixed basis set scheme uses the 6-311++G (2df,pd) basis set to describe the surface dimer silicon atoms and the benzonitrile molecule, and the 6-31G(d) basis set to describe the subsurface atoms and the terminating hydrogen atoms. The mixed basis set scheme serves to enhance the accuracy of the electronic structure of the chemically active atoms while minimizing computational costs. The energies reported have been corrected by zero-point energy under the same level of theory.

Results and Discussion

Theoretical results of activation barriers, adsorption energies, and desorption half-lives are summarized in Table 1. Desorption half-lives are estimated by kinetic analysis using a typical preexponential factor of 10^{13} for surface reactions.[43] Because the preexponential factor of 10^{13} is not significant certainty, we also calculate desorption half-lives with the preexponential factors of 10^{11} and 10^{15}. From the table, it can be concluded that the tendency of results with the three different preexponential factors are very similar. In our following discussion, we will use the results with 10^{13} to discuss our computations.

A. C≡N and C2═C1−C≡N [4 + 2] Cycloaddition Reactions. To quantitatively explore the competition of the reactivities of different functional groups of benzonitrile, initially, we have calculated the reaction pathways for reactions between a cyano group and the Si(100)-2×1 surface. The initial step of cyano group surface reactions involves the formation of a dative bond with the nitrogen atom of the cyano group on top of the down silicon atom of the surface dimer. The exothermicity calculated for adsorption energy of the dative-bonded state relative to the isolated benzonitrile and bare Si_9H_{12} cluster model is 17.75 kcal/mol. The formation of such a dative bond is barrierless through a nucleophilic attack of the lone pair of nitrogen atom toward the electrophilic down silicon atom of the surface dimer. Application of simple first-order kinetics analysis reveals that the desorption half-life of the dative-bonded state is 0.7 s, indicating the dative bond is not stable at room temperature.

Hence, the dative-bonded state of benzonitrile can work as a precursor to both C≡N [2 + 2] cycloaddition and C2═C1−C≡N [4 + 2] cycloaddition. The calculated reaction pathways at the Si(100)-2×1 surface are shown in Figure 2. For C≡N

TABLE 1: Theoretical Results for Benzonitrile at the Si(100)-2×1 Surface

	activation energy (kcal/mol)	adsorption energy (kcal/mol)	desorption half-lives[c] (s)		
			10^{11}	10^{13}	10^{15}
dative-bonded state	0	17.75	70	0.7	7.0×10^{-3}
C≡N [2 + 2] cycloaddition	9.2[a]	30.99	3.0×10^{11}	3.0×10^{9}	3.0×10^{7}
C2−C1−C≡N [4 + 2] cycloaddition	18.6[a]	7.00	9.0×10^{-7}	9.0×10^{-9}	9.0×10^{-11}
C1═C2 [2 + 2] cycloaddition	18.86	0.62	2.0×10^{-11}	2.0×10^{-13}	2.0×10^{-15}
C2═C3 [2 + 2] cycloaddition	17.46	5.91	1.4×10^{-7}	1.4×10^{-9}	1.4×10^{-11}
C3═C4 [2 + 2] cycloaddition	15.66	4.71	1.9×10^{-8}	1.9×10^{-10}	1.9×10^{-12}
C1═C4 [4 + 2] cycloaddition	6.32	16.59	9.4	9.4×10^{-2}	9.4×10^{-4}
C2═C5 [4 + 2] cycloaddition	4.46	21.26	2.5×10^{6}	2.5×10^{4}	2.5×10^{2}
o-C2−H dissociation	24.2	43.4	3.8×10^{22}	3.8×10^{20}	3.8×10^{18}
m-C3−H dissociation	22.5	44.8	4.0×10^{23}	4.0×10^{21}	4.0×10^{19}
p-C4−H dissociation	21.97	44.1	1.2×10^{23}	1.2×10^{21}	1.2×10^{19}
tight-bridge[3,4,5,6]	19.53[b]	34.08	5.8×10^{13}	5.8×10^{11}	5.8×10^{9}
tight-bridge[1,6,5,4]		30.05	6.5×10^{10}	6.5×10^{8}	6.5×10^{6}
tight-bridge[2,1,6,5]		30.26	9.3×10^{10}	9.3×10^{8}	9.3×10^{6}

[a] Relative to the dative-bonded state. [b] Relative to C2═C5 [4 + 2] at the two-dimers cluster. [c] Calculated at 300 K.

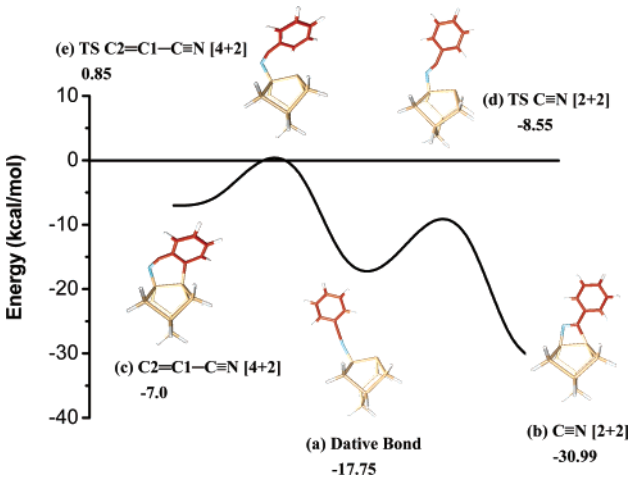

Figure 2. Reaction pathways of dative benzonitrile at the Si(100)-2×1 surface: (a) dative bond; (b) C≡N [2 + 2] cycloaddition; (c) C2−C1−C≡N [4 + 2] cycloaddition; (d) transition state for C≡N [2 + 2] cycloaddition; (e) transition state for C2−C1−C≡N [4 + 2] cycloaddition. Silicon atoms are in gold, nitrogen atoms are in blue, carbon atoms are in red, and hydrogen atoms are in white.

[2 + 2] cycloaddition, the dative-bonded state overcomes an activation barrier of 9.2 kcal/mol, leading to a four-membered heteroring product with adsorption energy of 30.99 kcal/mol below the vacuum level. Contrarily, C2═C1−C≡N [4 + 2] cycloaddition gets over a higher activation barrier of 18.6 kcal/mol, which results in a six-membered heteroring product, 7.0 kcal/mol below the vacuum level.

The results of simple kinetics analysis in Table 1 reveals that the surface products at the Si(100)-2×1 surface have desorption half-lives of 3×10^9 s and 0.9 μs for C≡N [2 + 2] product and C2═C1−C≡N [4 + 2] products, respectively. The 0.9 μs is much shorter than the time scale of the experiment, which indicates that the C2═C1−C≡N [4 + 2] surface product cannot be detected as a stable surface product. The bond angle of the two consecutive double bonds of C═C and C═N in the six-membered ring of the C2═C1−C≡N [4 + 2] product is 160° in optimized structure at the B3LYP/6-31G(d) theory level, causing larger strain in the heteroring and resulting in an unstable surface structure. To conclude, the C2═C1−C≡N [4 + 2] product can be excluded from stable surface products.

B. C═C Cycloaddition. The profiles of the [2 + 2] cycloaddition pathways via C═C of π-conjugated aromatic ring and the geometries associated with the critical points are shown in Figure 3. It is clear that there are three different C═C [2 + 2] cycloaddition reactions: C1═C2 [2 + 2] cycloaddition, C2═C3 [2 + 2] cycloaddition, and C3═C4 [2 + 2] cycloaddition. Our calculations show that the C═C [2 + 2] reactions undergo direct cycloaddition through activation energies of 18.86, 17.46, and 15.66 kcal/mol in sequence. The calculated adsorption energies of cycloaddition reactions are 0.62, 5.91, and 4.71 kcal/mol for C1═C2 [2 + 2] cycloaddition, C2═C3 [2 + 2] cycloaddition, and C3═C4 [2 + 2] cycloaddition, respectively.

Apart from the C═C [2 + 2] cycloaddition reactions, we have also calculated the C═C [4 + 2] cycloaddition reactions of the π-conjugated aromatic ring. Analogously, C═C [4 + 2] cycloaddition reactions also directly form the [4 + 2]-like products, as shown in Figure 4. C1═C4 [4 + 2] product binds at the surface dimer through two carbon atoms of the 1 and 4 positions of the phenyl ring. C2═C5 [4 + 2] product is bonded through the 2 and 5 carbon atoms of the phenyl ring. The calculated adsorption energy of C2═C5 [4 + 2] is 21.26 kcal/

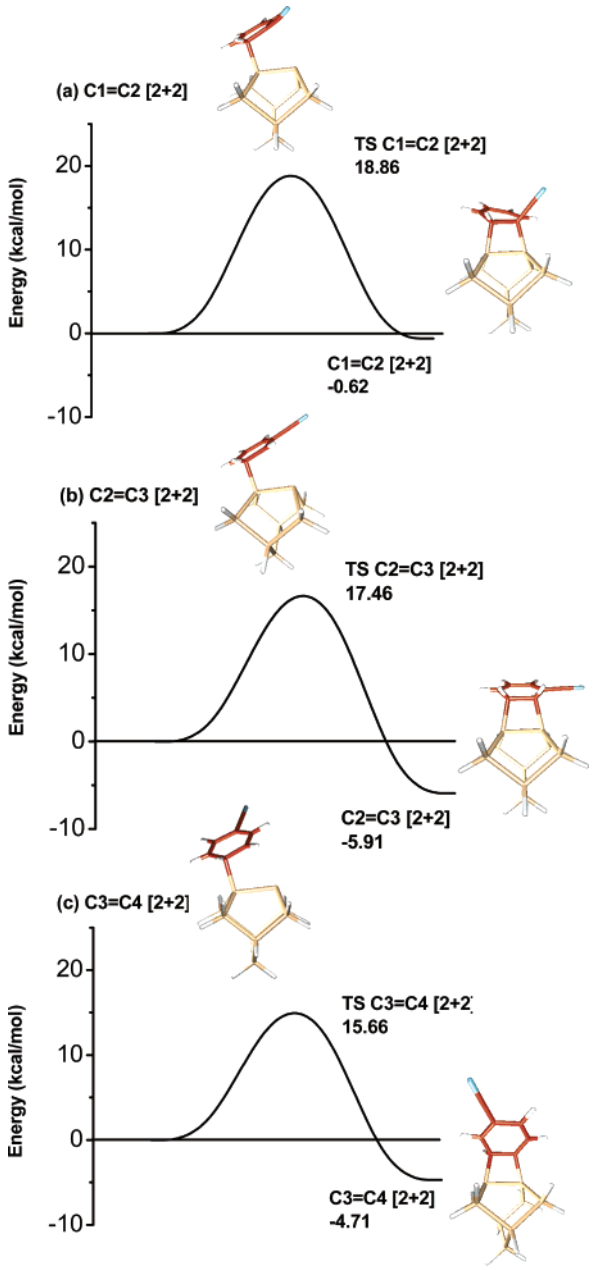

Figure 3. Reaction pathways of benzonitrile through C═C [2 + 2] cycloaddition at the Si(100)-2×1 surface: (a) C1═C2 [2 + 2] cycloaddition; (b) C2═C3 [2 + 2] cycloaddition; (c) C3═C4 [2 + 2] cycloaddition. Silicon atoms are in gold, nitrogen atoms are in blue, carbon atoms are in red, and hydrogen atoms are in white.

mol below the vaccum level, larger than that of C1═C4 [4 + 2] (16.59 kcal/mol below the vaccum level). The activation barrier of the C1═C4 [4 + 2] reaction is larger than that of the C2═C5 [4 + 2] reaction by 1.86 kcal/mol. The steric hindrance and directing effect of the cyano group can account for the differences in activation energies.

In both C═C [4 + 2] and C═C [2 + 2] cycloaddition reactions, two carbon atoms of the phenyl ring directly bond to the surface dimer and turn into sp^3 hybridization indeed, resulting in a loss of aromaticity. Our results of desorption half-lives in Table 1 clearly illustrate that the products of C═C [2 + 2] cycloaddition reactions and C1═C4 [4 + 2] cycloaddition reaction are unstable at the Si(100)-2×1 surface. In addition, C═C [2 + 2] cycloaddition reactions, at least, overcome an activation barrier of 15.0 kcal/mol, which is much higher than that of C═C [4 + 2] cycloaddition reactions. For

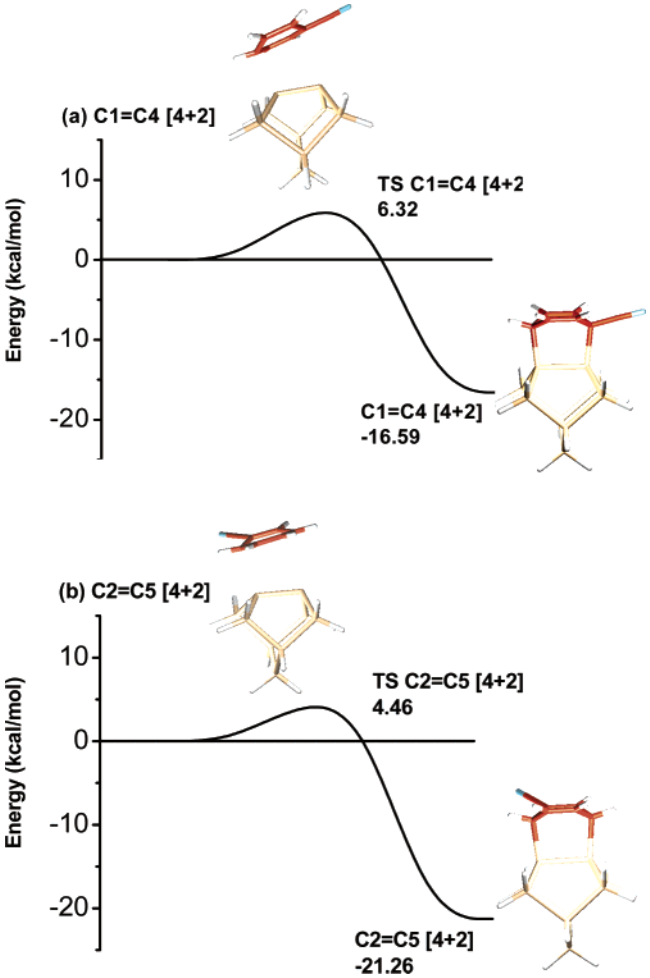

Figure 4. Reaction pathways of benzonitrile through C═C [4 + 2] cycloaddition at the Si(100)-2×1 surface: (a) C1═C4 [4 + 2] cycloaddition; (b) C2═C5 [4 + 2] cycloaddition. Silicon atoms are in gold, nitrogen atoms are in blue, carbon atoms are in red, and hydrogen atoms are in white.

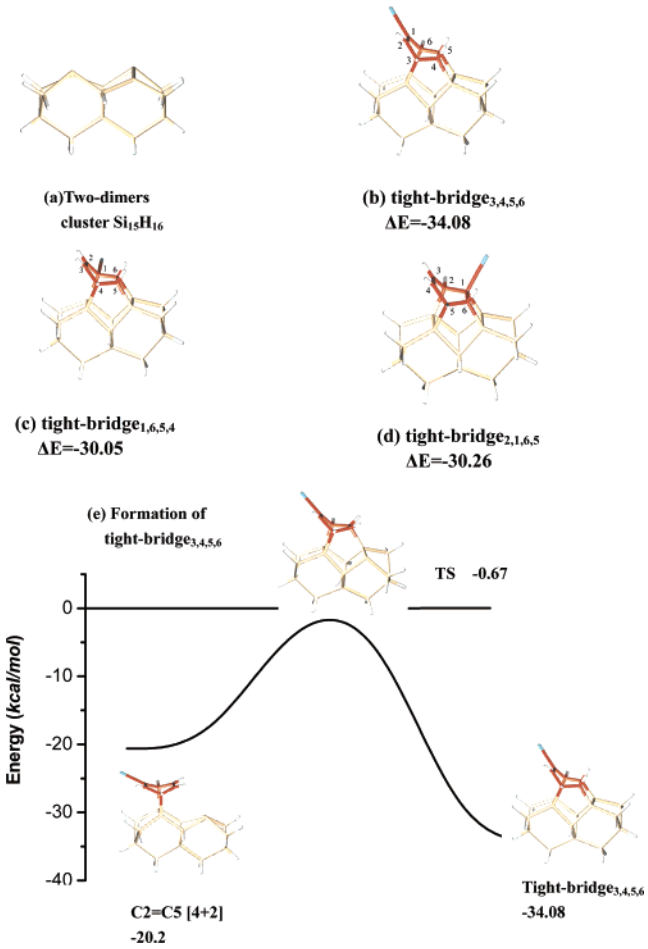

Figure 5. (a) Two-dimers cluster $Si_{15}H_{16}$; (b) tight-bridge$_{3,4,5,6}$ structure; (c) tight-bridge$_{1,6,5,4}$ structure; (d) tight-bridge^{2,1,6,5} structure; and (e) reaction pathway of the formation of tight-bridge^{3,4,5,6} structure.

C═C [4 + 2], the product fits the geometry imposed by the outward-pointing silicon dangling bonds; the C═C [4 + 2] surface reaction forms a stronger bond than the C═C [2 + 2] surface reaction. In addition, the delocalized nature of the cyclic π-electron wave functions of the phenyl ring of the pyridine molecule must be broken to form the surface adduct. The loss of resonance energy is approximately 30 kcal/mol for the phenyl ring, sufficient to destabilize the weakly bound C═C [2 + 2] cycloaddition products and C1═C4 [4 + 2] cycloaddition products.

In previous investigations on benzene at the Si(100)-2×1 surface, the [4 + 2] cycloaddition product can convert into a tight-bridge structure when adjacent surface dimers are unoccupied in an experimental time scale, indicating an activation energy of 23 kcal/mol around.[21,44−46] The tight-bridge structures of benzonitrile at the Si(100)-2×1 surface and the calculated reaction pathway for the formation of the tight-bridge^{3,4,5,6} are shown in Figure 5. Our calculations begin with the C2═C5 [4 + 2] product at two adjacent dimers at a dimer row (Figure 5a) and show the C2═C5 [4 + 2] surface structure at the two-dimers cluster overcomes an energy barrier of 19.53 kcal/mol to form the tight-bridge^{3,4,5,6} structure. According to our calculations of C═C [2 + 2] reactions, the discrepancy of energy barriers at different reaction sites at the phenyl ring is below 3.5 kcal/mol. Therefore, the difference of activation barriers for the formation of tight-bridge structures should be similar.

C. C−H Dissociative Reactions. Figure 6 shows the calculated C−H dissociation pathways along the reaction coordinate with critical points on the potential energy surface for the ortho, meta, and para carbon atoms of the phenyl ring. Our calculations indicate that the C−H dissociation reactions result in the most stable products, while the activation barriers are the highest among all possible reaction pathways. These dissociation reactions are direct pathways, leading to the attachment of benzonitrile at one of its ring carbon atoms at the Si(100)-2×1 surface. The carbon atom directly involved in binding to the silicon atom of the surface dimer becomes sp^3 hybridized at the transition state, resulting in the loss of aromaticity that can account for the high activation barrier of the C−H dissociation. Compared to the activation barrier of C≡N [2 + 2] cycloaddition, the branching ratio of C≡N [2 + 2] cycloaddition versus *p*-C4−H dissociation is 2.9×10^{25} and 2.1×10^{9}, at 110 and 300 K, respectively, if the surface reactions are irreversible. Therefore, the population of the C−H dissociation products is far below the detection limit of high-resolution electron energy loss spectroscopy (HREELS). In addition, the identical peak shape and peak position for C−H in-plane stretching modes were observed in both the chemisorbed and physisorbed benzonitrile, indicating that the retention of the sp^2 C−H vibrational feature and the absence of the rehybridization of carbon atoms in phenyl ring.[28] Moreover, the vibrational frequency (stretching mode) of around 2110 cm^{-1} for the monohydride species (Si−H) was not detected in HREEL spectra, further supporting for the absence of surface reaction products via C−H dissociation.

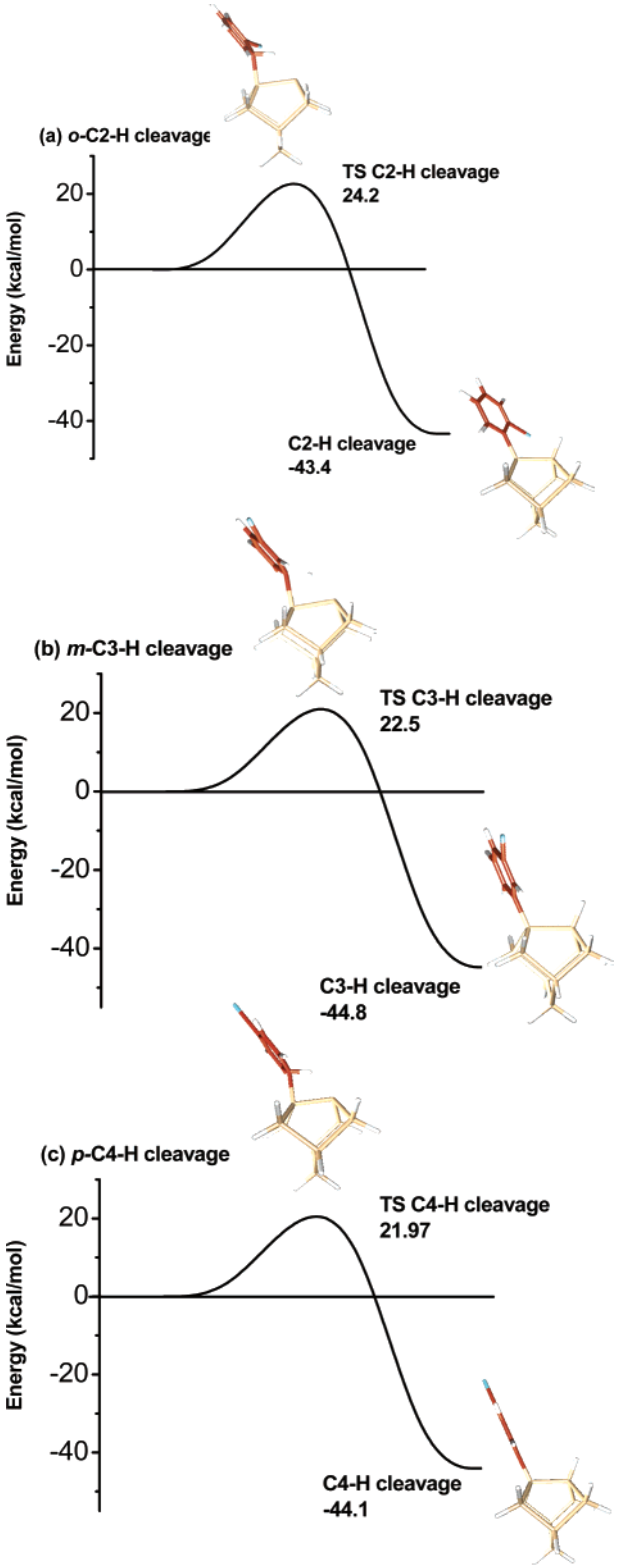

Figure 6. Reaction pathways of benzonitrile through C−H cleavage at the Si(100)-2×1 surface: (a) *o*-C2−H cleavage; (b) *m*-C3−H cleavage; (c) *p*-C4−H cleavage. Silicon atoms are in gold, nitrogen atoms are in blue, carbon atoms are in red, and hydrogen atoms are in white.

D. Selectivity and Competition. In Tao et al.'s work,[28] The characteristic vibrational modes of monosubstituted benzene, the γ(C−H) peak around 750 cm^{-1} and the ν(C−C) peaks around 1560−1615 and 1450−1525 cm^{-1}, were retained, indicating an intact phenyl ring. The characteristic peak around 2267 cm^{-1} of ν(C≡N) was not observed for chemisorbed benzonitrile in the HREEL spectra and substituted by the vibration of the stretching mode of C═N around 1629 cm^{-1}, suggesting that the nitrile functional group participates in the surface reaction. Ultraviolet photoelectron spectroscopy (UPS) also suggested that only the cyano group interacted with the Si(100)-2×1 surface. These experimental results suggest that carbon atoms of the phenyl ring do not participate in the surface reactions, maintaining an intact phenyl ring skeleton and aromaticity in the chemisorbed benzonitrile.

According to our calculations, the C≡N [2 + 2] cycloaddition product, the C2═C5 [4 + 2] product, and the tight-bridge products may be observed at the Si(100)-2×1 surface. When the reaction pathways of C≡N [2 + 2] and C2═C5 [4 + 2] are compared, our calculations show that the C2═C5 [4 + 2] cycloaddition reaction has a lower activation barrier, while the C≡N [2 + 2] cycloaddition product is a more stable surface adduct. However, the C2═C5 [4 + 2] structure results in the loss of aromaticity. The loss of aromaticity will weaken binding energy and hence lower barriers to desorption due to the loss of resonance. This destablilization may be sufficient to cause the reversible desorption of the C2═C5 [4 + 2] product. Thus, the more thermodynamically C≡N [2 + 2] product can form, even if the formation of C≡N [2 + 2] is less kinetically (but still accessible). Therefore, the C2═C5 [4 + 2] cycloaddition product is not detected at the Si(100)-2×1 surface. When tight-bridge structures that occur from the [4 + 2] cycloaddition reactions are compared, the adsorption energy of the C≡N [2 + 2] product is close to those of tight-bridge structures. Because of the high activation barriers for the formation of tight-bridge structures and the loss of resonance energy, the tight-bridge structures can be ruled out of the observed surface species. Therefore, the cycloaddition reaction via nitrile functional group is the selective reaction pathway of the benzonitrile molecule at the Si(100)-2×1 surface. The results of the vibrational frequencies of our calculations of C≡N [2 + 2] cycloaddition structure and HREELS experiments are in good agreement (listed in the Supporting Information).

Conclusions

In this work, we have used density functional theory with the Si_9H_{12} one-dimer cluster model to investigate detailed reaction mechanisms of adsorption and dissociation of benzonitrile at the Si(100)-2×1 surface. Our calculations show that C−H dissociative configurations are the most stable products at the surface, but the activation barriers are the highest. C═C [2 + 2] products are unstable at the surface because of large activation barriers and low adsorption energies. The C2−C1−C≡N [4 + 2] and C1═C4 [4 + 2] are also unstable for low adsorption energies. Therefore, our calculations predict that the C≡N [2 + 2] product, the C2═C5 [4 + 2] product, and the tight-bridge structures may result in a mixture of products. The loss of resonance stabilization energy for the C2═C5 [4 + 2] cycloaddition product and tight-bridge products result in destabilizing these products and leading to a selective C≡N [2 + 2] surface structure at the Si(100)-2×1 surface. The theoretical results show good agreement with experimental results. Therefore, chemisorbed benzonitrile contains an intact phenyl ring protruding from the surface, providing a platform to attach additional organic molecules through typical phenyl ring reactions.

Acknowledgment. This work was supported by NKBRSF (Grant 1999075302), the Knowledge Innovation Program of the Chinese Academy of Sciences (Grant INF105-SCE-02-08), and

NSFC (Grants 20373071, 20333050). The authors thank Jing Li for insightful discussion.

Supporting Information Available: Table of comparison of the calculated vibrational frequencies in our work and the measured vibrational frequencies. This material is available free of charge via the Internet at http://pubs.acs.org.

References and Notes

(1) Yates, J. T., Jr. *Science* **1998**, *278*, 335.
(2) Ruda, H. E. *Science* **1999**, *283*, 646.
(3) Lopinski, G. P.; Wayner, D. D. M.; Wolkow, R. A. *Nature* **2000**, *406*, 48.
(4) Hamers, R. J. *Nature* **2001**, *412*, 489.
(5) Lin, Z.; Strother, T.; Cai, W.; Cao, X. P.; Smith, L. M.; Hamers, R. J. *Langmuir* **2002**, *18*, 788.
(6) Waltenburg, H. N.; Yates, J. T., Jr. *Chem. Rev.* **1995**, *95*, 1589.
(7) Hamers, R. J.; Wang, Y. *Chem. Rev.* **1996**, *96*, 1261.
(8) Wolkow, R. A. *Annu. Rev. Phys. Chem.* **1999**, *50*, 413.
(9) Buriak, J. M. *Chem. Commun. (Cambridge)* **1999**, 1051.
(10) Hamers, R. J.; Coulter, S. K.; Ellison, M. D.; Hovis, J. S.; Padowitz, D. F.; Schwartz, M. P.; Greenlife, C. M.; Russell, J. N., Jr. *Acc. Chem. Res.* **2000**, *33*, 617.
(11) Bent, S. F. *Surf. Sci.* **2002**, *500*, 879.
(12) Bent, S. F. *J. Phys. Chem. B* **2002**, *106*, 2830.
(13) Lu, X.; Lin, M. C. *Int. Rev. Phys. Chem.* **2002**, *21*, 137.
(14) Bent, S. F. *Prog. In Surf. Sci.* **2003**, *73*, 1.
(15) Hata, K.; Kimura, T.; Ozawa, S.; Shigekawa, H. *J. Vac. Sci. Technol., A* **2000**, *18*, 1933.
(16) Duke, C. B. *Chem. Rev.* **1996**, *96*, 1237.
(17) Lopinski, G. P.; Fortier, T. M.; Moffatt, D. J.; Wolkow, R. A. *J. Vac. Sci. Technol., A* **1998**, *16*, 1037.
(18) Self, K. W.; Pelzel, R.; Owen, J. H. G.; Yan, C.; Widdra, W.; Weinberg, W. H. *J. Vac. Sci. Technol., A* **1998**, *16*, 1031.
(19) Kong, M. J.; Teplyakov, A. V.; Lyubovitsky, J. G.; Bent, S. F. *Surf. Sci.* **1998**, *411*, 286.
(20) Taguchi, Y.; Ohta, Y.; Katsumi, T.; Ichikawa, K.; Aita, O. *J. Electron. Spectrosc.* **1998**, *88*, 671.
(21) Wolkow, R. A.; Lopinski, G. P.; Moffatt, D. J. *Surf. Sci.* **1998**, *416*, L1107.
(22) Hofer, W. A.; Fisher, A. J.; Lopinski, G. P.; Wolkow, R. A. *Surf. Sci.* **2001**, *482*, 1181.
(23) Schwartz, M. P.; Ellison, M. D.; Coulter, S. K.; Hovis, J. S.; Hamers, R. J. *J. Am. Chem. Soc.* **2000**, *122*, 8529.
(24) Bitzer, T.; Alkunshalie, T.; Richardson, N. V. *Surf. Sci.* **1996**, *368*, 202.
(25) Kugler, T.; Thibaut, U.; Abraham, M.; Folkers, G.; Gopel, W. *Surf. Sci.* **1992**, *260*, 64.
(26) Rummel, R. M.; Ziegler, C. *Surf. Sci.* **1998**, *418*, 303.
(27) Ellison, M. D.; Hamers, R. J. *J. Phys. Chem. B* **1999**, *103*, 6243.
(28) Tao, F.; Wang, Z. H.; Xu, G. Q. *J. Phys. Chem. B* **2002**, *106*, 3557.
(29) Coulter, S. K.; Schwartz, M. P.; Hamers, R. J.*J. Phys. Chem. B* **2001**, *105*, 3079.
(30) Tao, F.; Sim, W. S.; Xu, G. Q.; Qiao, M. H. *J. Am. Chem. Soc.* **2001**, *123*, 9397.
(31) Tao, F.; Chen, X. F.; Wang, Z. H.; Xu, G. Q. *J. Phys. Chem. B* **2002**, *106*, 3890.
(32) Choi, C. H.; Gordon, M. S. *J. Am. Chem. Soc.* **2002**, *124*, 6162.
(33) Lu, X.; Xu, X.; Wu, J. M.; Wang, N. Q.; Zhang, Q. *New J. Chem.* **2002**, *26*, 160.
(34) Filler, M. A.; Mui, C.; Musgrave, C. B.; Bent, S. F. *J. Am. Chem. Soc.* **2003**, *125*, 4928.
(35) Mui, C.; Filler, M. A.; Bent, S. F.; Musgrave, C. B. *J. Phys. Chem. B* **2003**, *107*, 12256.
(36) Widjaja, Y.; Musgrave, C. B. *Surf. Sci.* **2000**, *406*, 9.
(37) Becke, A. D. *J. Chem. Phys.* **1993**, *98*, 1372.
(38) Becke, A. D. *J. Chem. Phys.* **1993**, *98*, 5648.
(39) Lee, C.; Yang, W.; Parr, R. G. *Phys. Rev. B* **1988**, *37*, 785.
(40) Hohenberg, P.; Kohn, W. *Phys. Rev.* **1964**, *136*, B864.
(41) Kohn, W.; Sham, L. J. *Phys. ReV.* **1965**, *140*, A1133.
(42) Frisch, M. J.; Trucks, G. W.; Schlegel, H. B.; Scuseria, G. E.; Robb, M. A.; Cheeseman, J. R.; Z akrzewski, V. G.; Montgomery, J. A., Jr.; Stratmann, R. E.; Burant, J. C.; Dapprich, S.; Millam, J. M.; Daniels, A. D.; Kudin, K. N.; Strain, M. Pomelli, C.; Adamo, C.; Clifford, S.; Ochterski, J.; Petersson, G. A.; Ayala, P. Y.; Cui, Q.; Morokuma, K.; Malick, D. K.; Rabuck, A. D.; Raghavachari, K.; Foresman, J. B.; Cioslowski, J.; Oritz, J. V.; Stefanov, B. B.; Liu, G.; Liashenko, A.; Piskorz, P.; Komaromi, I.; Gomperts, R.; Martin, R. L.; Fox, D. J.; Keith, T.; Al-Laham, M. A.; Peng, C. Y.; Nanayakkara, A.; Gonzalez, C.; Challacombe, M.; Gill, P. M. W.; Johnson, B. G.; Chen, W.; Wong, M. W.; Andres, J. L.; Head-Gordon, M.; Replogle, E. S.; Pople, J. A. *Gaussian 98W*; Gaussian, Inc.: Pittsburgh, PA, 1998.
(43) Baetzold, R. C.; Somorjai, G. A. *J. Catal.* **1976**, *45*, 94.
(44) Schwartz, M. P.; Ellison, M. D.; Coulter, S. K.; Hovis, J. S.; Hamers, R. J. *J. Am. Chem. Soc.* **2000**, *122*, 8529.
(45) Lopinski, G. P.; Moffatt, D. J.; Wolkow, R. A. *Chem. Phys. Lett.* **1998**, *282*, 305.
(46) Hofer, W. A.; Fisher, A. J.; Lopinski, G. P.; Wolkow, R. A. *Phys. Rev. B* **2001**, *63*, 5314.